JOURNAL OF AGRICULTURAL AND FOOD CHEMISTRY

Food Safety and Toxicology

Sulforaphane rescues the ethanol-suppressed angiogenesis through oxidative- and ER-stress in chick embryos

Guang Wang, Jia-hui Nie, Yongping Bao, and Xuesong Yang

J. Agric. Food Chem., **Just Accepted Manuscript** • DOI: 10.1021/acs.jafc.8b02949 • Publication Date (Web): 20 Aug 2018

ACS Publications

is published by the American Chemical Society. 1155 Sixteenth Street N.W., Washington, DC 20036

Sulforaphane rescues the ethanol-suppressed angiogenesis through oxidative- and ER-stress in chick embryos

Guang Wang[†, §, ⊥], *Jia-hui Nie*[†, §, ⊥], *Yongping Bao**[‡], *Xuesong Yang**[†, §]

[†]*Key Laboratory for Regenerative Medicine of the Ministry of Education, Division of Histology and Embryology, Medical College, Jinan University, Guangzhou 510632, China*

[‡]*Norwich MedicalSchool, University of East Anglia, Norwich, Norfolk, NR4 7UQ, UK*

[§]*International Joint Laboratory for Embryonic Development & Prenatal Medicine,MedicalCollege, JinanUniversity, Guangzhou 510632, China*

[⊥]*contribute to the work equally*

**The corresponding authors：Xuesong Yang. E-mail: yang_xuesong@126.com; or Yongping Bao. E-mail:Y.Bao@uea.ac.uk*

Abstract

Our previous study showed that ethanol exposure inhibited embryonic angiogenesis mainly due to the excessive stimulation of reactive oxygen species (ROS) production. In this study, we investigated whether sulforaphane (SFN), a known dietary bioactive compound, could ameliorate the ethanol-suppressed angiogenesis using chick embryo angiogenesis models. Using chick YSM (yolk sac membrane) and CAM (chorioallantoic membrane) models, we demonstrated that low concentrations of SFN (2.5-10 μM) administration alone increased angiogenesis, but high concentrations of SFN (20-40 μM) inhibited angiogenesis. SFN administration alleviated ethanol-suppressed angiogenesis and angiogenesis-related gene expressions in both angiogenesis models. Ethanol exposure caused cell apoptosis in chick CAM, and the cells apoptosis could be remitted by administration of SFN. Subsequently, we demonstrated that ethanol-induced increase of ROS and antioxidant enzymes activity reduction were rescued partially by SFN. Similar results were obtained in ER stress determination indicated by ATF6 and GRP78 expression or thapsigargin-induced ER stress in the presence or absence of SFN. Taken together, our experiments show that SFN administration can ameliorate - ethanol-suppressed embryonic angiogenesis, and this is mainly achieved by alleviating excessive ROS production and ER stress. This study suggested that SFN, in appropriate concentrations, could be a potential candidate compound for preventing negative impact of alcohol on angiogenesis.

Key words: Sulforaphane, ethanol, embryonic angiogenesis, chick CAM/YSM, oxidative stress, ER stress

Introduction

Fetal alcohol spectrum disorder (FASD) is exhibited as birth defects induced by alcohol consumption by pregnant women during pregnancy. The physical developmental disorders include facial deformities, skeletal defects and cardiovascular irregularities [1-2], in which the severe cardiovascular deformation can be lethal to the embryo, so that it instead appears more in neonates [3]. A functional cardiovascular system is firstly developed during embryogenesis, because of the crucial role of the vasculature and heart in developing embryos [4]. Both vasculogenesis and angiogenesis will be completed before the prenatal period. Angiogenesis involves the expansion and remodeling of the vascular plexus via endothelial sprouting and intussusceptive microvascular growth [5], which is a complex process and regulated by a significant number of modulators. Among them is vascular endothelial growth factor (VEGF), which is a specific mitogen, stimulates vasculogenesis and angiogenesis through binding to VEGF receptors [6]. Fibroblast growth factor 2 (FGF2), known for its angiogenic potential, is also of great importance in angiogenesis, because it can promote endothelial cell proliferation and the physical organization of endothelial cells into tube-like structures [7]. Hypoxia is considered as an indispensable factor in pathological angiogenesis, since hypoxia can activate the vital angiogenesis mediators such as transcription factors hypoxia-inducible factor (HIF) and VEGF [8-9]. Alcohol can pass through the placenta and damage the developing embryos and fetus. Our previous work revealed that maternal ethanol exposure inhibited embryonic angiogenesis through promoting superfluous reactive oxygen species (ROS)

production during chick embryo development [10]. Therefore, a novel approach for prevention of fetal alcohol spectrum is certainly in demand.

As a component of oxidative phosphorylation, ROS play an important role in the redox control of various signaling pathways [11-13]. ROS could function as primary or secondary messengers to influence embryonic development through promoting cell growth or death, and positive or negative feedback. However, excessive ROS generation is associated with the pathogenesis of many diseases [11-13], since ROS accumulation would interfere with normal cellular functions through the deleterious oxidization on proteins, lipids, DNA and signal transduction [14]. Furthermore, accumulated data show that oxidative stress is closely associated with endoplasmic reticulum (ER) stress, and that ROS could be generated as by product during protein folding [15]. Therefore, a fine balance between ROS production and degradation is indispensable for maintaining physiological functions [16-17].

Sulforaphane ([1-isothiocyanato-4-(methyl-sulfinyl) butane], SFN), is the most extensively studied isothiocyanate (ITC). ITCs are derived from their precursors glucosinolates under the action of myrosinase. SFN is found at high levels in cruciferous vegetables such as broccoli and cauliflower, and has been reported to exert a variety of bio-active effects including anti-oxidation, anti-inflammation, cytotoxicity and cytoprotection and anti-angiogenesis [18-19]. SFN is an organosulfur compound in cruciferous vegetables, and SFN's anticarcinogenic properties have been well documented, which acts through the induction of phase II detoxifying enzymes [20]. SFN could exert anticarcinogenic effects through its antioxidant or electrophile

response element-regulated phase 2 enzyme and antioxidant genes activating the signaling pathway of nuclear factor-E2-related factor 2 (Nrf2)-Kelch-like ECH-associated protein 1 (Keap1) [21-22]. The induction of Nrf2 protects normal cells from free-radical mediated oxidative stress via upregulation of chemoprotective genes and phase II enzymes, and induction of apoptosis [23-24]. Whether or not SFN is able to enhance endogenous antioxidative capacity against free-radical damage in embryonic angiogenesis has not been fully investigated [1].

Thus, the hypothesis that SFN ameliorates ethanol exposure-induced repression of embryonic angiogenesis is explored and corresponding mechanisms are studied using *in vivo* chick yolk sac membrane (YSM) and chorioallantoic membrane (CAM) models, which have been proved to be the effective models for this type of study [10, 25-26].

Materials and methods

Avian embryos and treatments

Fertilized chick eggs were obtained from the Avian Farm of the South China Agriculture University. To administer DMSO (control), SFN (Sulforaphane, Sigma-Aldrich, MO, USA) or ethanol to chick embryos YSM, 40 μl DMSO (0.018%, Sigma-Aldrich, MO, USA), SFN (2.5, 5, 10, 20, and 40 μM) and/or ethanol (15%) were directly added into plastic rings every 12 hours as shown in Fig. 1A. The treated embryos were incubated at 38 ℃ for the desired times based on the experimental requirement. To administer DMSO (control), SFN, ethanol or thapsigargin to chick embryos CAM, 200 μl DMSO, various concentrations of SFN (2.5 μM, 5 μM, 10 μM), ethanol (15%) or thapsigargin (1 μM, Sigma-Aldrich, MO, USA) were directly injected into the air chamber at the blunt end of the fertilized egg every three days as shown in Fig. 2A. The eggs were sealed and incubated at 38 ℃ until day 9 (E9.0) for harvest. All of the harvested YSM and CAM were photographed using a stereomicroscope (Olympus MVX10, Tokyo, Japan) before they were fixed with 4% paraformaldehyde for analysis of morphology and gene expression. Only the surviving embryos were used for the further research.

Cell culture and tube formation assay

Human umbilical vascular endothelial cells (HUVECs) were a kindly gift from Zhi Huang's lab, and cultured in Dulbecco's modified Eagle's medium (DMEM) medium (Gibco, Shanghai, China) supplemented with 10% fetal bovine serum (FBS),

and incubated at 37 °C and 5% CO_2. The tube formation assay was performed as follows. Each well of 24-well plates were coated with 300 μL Matrigel (BD Bioscience, NJ, USA) and incubated at 37 °C for 30 min to promote gelling. HUVECs were resuspended in DMEM medium (serum concentration 10%) and simultaneously seeded with DMSO or SFN (1.25 μM) and/or ethanol (1%) in matrigel coated plates in a final volume of 1 ml (2.5×10^5 cells per well). Then the images were taken using an inverted microscope (Nikon Eclipse Ti-U, Tokyo, Japan) at the middle version of the each well at 4 h and 8 h. After 8 h, the plates were fixed with 4% paraformaldehyde, immunofluorescent stained with CD31 (1:200, Abcam, MA, USA) and counterstained with DAPI. Each well was tested in triplicate and each experiment was repeated at least 3 times. The total length of tube was calculated from examinations of 6 separate microscopic fields.

Histological analysis and immunofluorescent staining

For the histological analysis, the CAM or YSM were dehydrated, embedded in paraffin wax and serially sectioned at 5 μm using a microtome (Leica RM2126RT, Wetzlar, Germany). The sections were de-waxed in xylene, rehydrated and stained with either hematoxylin and eosin dye or immunofluorescent staining. The sections were photographed using a fluorescent microscope (Olympus IX50, Tokyo, Japan) with the NIS-Elements F3.2 software package.

Immunofluorescent staining was performed on some sections of the CAM and HUVECs, using a monoclonal primary antibody against caveolin 1 (Cav1, 1:200,

Santa Cruz, TX, USA), GRP78 (1:100, Abcam, MA, USA) or ATP6 (1:200, Abcam, MA, USA) at 4 °C overnight and treated with the Alexa Fluor 555 anti-rabbit IgG (1:500, Invitrogen, CA, USA) secondary antibody. The sections were counterstained with 4′-6-Diamidino-2-phenylindole (DAPI, 5 μg/mL; Life Tech, CA, USA) 20 min at 37 °C to reveal the nuclei and finally photographed by an Olympus IX51 microscope (Tokyo, Japan) or inverted microscope (Nikon Eclipse Ti-U, Tokyo, Japan).

Assessment of angiogenesis using chick CAM

As described previously [26], the CAM and accompanying blood vessels from the treated embryos were photographed using a Sony SLT-A55 camera (16.2M Pixels) with a Tamron 90mm F2.8 Macro lens. Ten embryos in each experimental group were examined. The CAM tissues from eight embryos in each group were embedded, sectioned and stained with hematoxylin & eosin. The blood vessel density (BVD) were quantified and analyzed. The areas occupied by the blood vessel plexus were quantified using an IPP 5.0 image analysis program. The blood vessel density was expressed as the percentage of area occupied by the blood vessel over the whole area under the microscopic field as described previously [25].

Western blotting

Western blotting was performed in accordance with standard procedures using antibodies which specifically recognized GRP78 (1:1000, Abcam, MA, USA). The protein was isolated from DMSO (control), SFN, ethanol and SFN+ethanol CAM

(E9.0 day) using a radio-immuno-precipitation assay (RIPA, Sigma-Aldrich, MO, USA) buffer supplemented with protease and phosphatase inhibitors. Protein concentrations were quantified with the BCA assay. The loading control was a β-actin antibody (1:3000, Proteintech, IL, USA). Quantity One (BIO-RAD, CA, USA) was used to capture the chemiluminescent signals and analyze the data. All samples were performed in triplicate.

RNA isolation and quantitative PCR

Total RNA was isolated from DMSO (control), SFN, ethanol, thapsigargin, SFN+ethanol and SFN+thapsigargin CAM (E9.0 day) using a Trizol kit (Invitrogen, CA, USA) according to the manufacturer's instructions. First-strand cDNA was synthesized to a final volume of 20 μl using iScript^{TM} cDNA Synthesis Kit (BIO-RAD, CA, USA). Following reverse transcription, PCR amplification of the cDNA was performed as described previously [27-28]. SYBR® Green qPCR assays were then performed using a PrimeScript^{TM} RT reagent kit (Takara, Shiga-ken, Japan). All specific primers used are shown in Supplementary Fig. 1. Reverse transcription and amplification reactions were performed in Bio-Rad S1000^{TM} (Bio-Rad, CA, USA) and ABI 7000 thermal cyclers, respectively. The expression of a non-variant housekeeping gene GAPDH was determined in parallel to confirm that equal amounts of RNA were used in each reaction. The ratio between the intensities of the fluorescently-stained bands corresponding to genes and GAPDH was calculated to quantify the level of the transcripts for those genes mRNAs.

185

186 ***TUNEL staining***

187 The chick CAM (E9.0 day) were fixed in Bouin's solution and paraffin-embedded.
188 Sections (5 μm) were deparaffinized and stained with *in situ* cell death detection kit
189 (Roche, Basel, Switzerland) according to the manufacturer's instructions. The extent
190 of cell death was quantified by counting $TUNEL^+$ cells on consecutive transverse
191 sections of treated and untreated CAM. The proliferation index was calculated
192 through counting TUNEL positive cells relative to the total cell numbers
193 (TUNEL-positive cells/total cell numbers).

194

195 ***Measurement of oxidative stress***

196 Intracellular ROS was determined using a non-fluorescent dye DCFH-DA
197 (2′7′-dichlorodihydrofluorescein diacetate) (Sigma-Aldrich, MO, USA), which is
198 oxidized by ROS to the fluorescent dye DCF (2′,7′-dichlorofluorescin). The YSM
199 tissues were collected from the plastic rings, minced with sterile scissors and digested
200 with trypsin eliminate obvious tissue mass. An equal volume of cell culture medium
201 was added to stop the digestion, the filtrate was collected after sieving (pore size 0.2
202 μm), and centrifuged and the medium discarded. The cells were resuspended in
203 medium, counted and the volume adjusted to give approximately 1×10^6 cells/ml. All
204 the above operations are performed at 4 °C. The control, ethanol and/or SFN groups
205 were incubated in 10 μM DCFH-DA at 37 °C for 20 minutes. Fluorescence was
206 measured with a Gallios flow cytometer under 488nm excitation wavelength

(Beckman Coulter, CA, USA).

Quantitation of apoptotic cells

Annexin V-FITC (BD Bioscience, NJ, USA) and PI double staining were used to identify and quantify apoptotic cells present in the control, ethanol and/or SFN groups. The YSM tissues were collected from the plastic rings and then cell samples were prepared as above for the detection of intracellular ROS by the DCFH-DA method. Briefly, the cells were collected and resuspended in cold PBS at a density of 1×10^6 cells/ml and then introduced into 200 μl of the Annexin V-binding buffer. The samples were then incubated with 2.5 μl FITC-labeled Annexin V and 2.5 μl PI at room temperature for 15 min in the dark and immediately analyzed by a Gallios flow cytometer (Beckman Coulter, CA, USA). The acquired data were evaluated using FCS-Express software version 3.0 (De Novo).

Measurement of T-SOD, GSH, GSSG, MDA, ADH and ALDH

For measuring the levels of T-SOD (total superoxide dismutase), GSH (glutathione)，GSSG (glutathione disulfide), MDA (malondialdehyde), ADH (alcohol dehydrogenase) and ALDH (aldehyde dehydrogenase) activity in tissue homogenate of the chick CAM (E9.0 day), corresponding commercial determination kits were conducted according to the standard procedures in the manufacturer's instructions. Detection kits for T-SOD activity and GSH, GSSG, MDA levels were provided from Jiancheng Corp (Nanjing, China) and detection kits for ADH and ALDH activities

were provided from Cominbio (Suzhou, China). Results of GSH, GSSG and MDA levels were expressed as μmol/g or nmol/g tissue, result of T-SOD activity was expressed as U/mg protein, and results of ADH and ALDH activities were expressed as nmol/min/mg protein. Protein concentrations were quantified with the BCA assay.

Data analysis

Statistical analysis for all the experimental data generated was performed using a Graphpad prism 5 statistical package program for Windows. The data were presented as average ± SD. Statistical significance were determined using paired t-tests, independent samples t-test or one-way analysis of variance (ANOVA). *$p<0.05$, **$p<0.01$ and ***$p<0.001$ indicate significant difference between control and ethanol and/or SFN treated specimens.

Results

SFN administration bilaterally affects the chick embryonic angiogenesis.

An embryonic angiogenesis model, chick YSM (yolk sac membrane) [10] was used to determine the effect of various concentrations of SFN administration alone on angiogenesis since it is straightforward to observe the angiogenesis through quantitatively measuring the blood vessel density of vascular plexuses in the plastic rings as shown in Fig. 1A. The photographs for each group were taken after incubation for 0 (Fig. 1B-G), 12 (Fig. 1B1-G1), 24 (Fig. 1B2-G2) and 36 (Fig. 1B3-G3) hours. The results showed that density of vascular plexuses increased in a dose-dependent manner within the SFN concentrations of 2.5 - 10 μM, but the densities of vascular plexuses dropped when SFN concentration was over 20 μM (Fig. 1). This tendency is similar for each time point (Fig. 1H).

Another angiogenesis model, chick CAM (chorioallantoic membrane), which has been widely employed as an *in vivo* angiogenesis model, was then used to confirm the role of 2.5 – 10 μM SFN on the promotion of angiogenesis [25]. Using the chick CAM as shown in Fig. 2A, we investigated the effect of different concentrations of SFN administration alone on angiogenesis. The body weight of embryos increased in a dose-dependent manner in the SFN groups (Fig. 2B), and 2.5 - 10.0 μM SFN did not induce embryo death (Fig. 2C). As shown in Fig. 1D, the vascular plexus densities increased with SFN concentration, particularly when SFN concentration reached 10 μM (Fig. 2E).

We have also investigated the effect of SFN on ethanol-repressed endothelial tube

formation in a 3-D angiogenesis assay (Fig S2). SFN at 1.25 μM promoted tube formation and 1% ethanol administration reduced it in compassion to control. Co-application of SFN could significantly rescued ethanol-reduced tube formation. The aforementioned data imply that SFN administration time- and dose-dependently rescued ethanol-repressed embryonic angiogenesis.

SFN administration time- and dose-dependently rescued ethanol-repressed embryonic angiogenesis.

Using the same strategy, the chick YSM angiogenesis model was employed to test what would happen when SFN was administrated together with ethanol as shown in Fig. 3A. The results revealed that SFN (5.0 μM and 10.0 μM) administration alone increased the vascular plexus densities in a time- and dose-dependent manner; ethanol administration alone decreased the vascular plexus densities in a time-dependent manner; the ethanol-induced reduction of vascular plexus densities was rescued by co-administration with SFN in a time- and dose-dependent manner (Fig. 3B-G, 3B1-G1, 3B2-G2, 3B3-G3, 3H).

Using the chick CAM model again, SFN was administrated together with ethanol (Fig. 4). The results showed that ethanol administrated alone decreased the vascular plexus densities on chick CAM and body weight compared to control, but this ethanol-induced reduction was dramatically rescued by co-administration of 10 μM SFN (Fig. 4A-E). Ethanol treatment resulted in the deaths of 55.70% of chick embryos, but this was reduced to 37.10% of chick embryo deaths on addition of 10

μM SFN after ethanol exposure (Fig. 4F). Likewise, we found that the ethanol-induced reduction of vascular plexus densities was rescued by the co-administration with SFN (Fig. 4G). The high magnification images which focused on the principal blood vessels on CAM showed that SFN administration raised vascular diameters in compassion to control; ethanol administration reduced the diameters of blood vessels; co-application of SFN could significantly rescued ethanol-reduced vascular diameters (Fig. 4A1-D1, H-K and P). This effect could be more distinctly observed in the Cav1 immunofluorescent staining (Fig. 4L-O). Quantitative PCR for VEGFa (Fig. 4Q), FGF2 (Fig. 4R) and HIF1α (Fig. 4S) determination showed that the expression of these genes in chick CAM likewise underwent similar alterations with combinational application of SFN significantly rescuing the ethanol-induced inhibition of gene expressions. The aforementioned data imply that SFN administration time- and dose-dependently rescued ethanol-repressed embryonic angiogenesis.

SFN administration retrieved the ethanol-induced cell apoptosis on chick CAM.

Using TUNEL assay kit, the cell apoptosis was determined on chick CAM exposed to SFN (10 μM), ethanol or in combination (Fig. 5). Histochemical staining showed that the TUNEL staining was enhanced by ethanol administration alone, but dropped when applied with SFN compared to ethanol administration alone (Fig. 5A-D and E), which could be reflected through counting the TUNEL positive individual cell numbers in the high magnification images (Fig. 5A1-D1). Moreover, flow cytometry

analysis (stained with Annexin V/PI) was employed to detect the cell apoptosis. The results showed that ethanol administration alone increased the apoptotic positive necrotic cells, but dropped significantly when combined with 5 μM and 10 μM SFN (Fig. 5F-G).

SFN administration alleviated the ethanol-induced oxidative stress and endoplasmic reticulum stress on chick CAM.

SFN at 5 μM or 10 μM or 15% ethanol administration alone lead to an increase of intercellular ROS production in chick CAM, but ROS production significantly dropped when SFN and ethanol were applied together (Fig. 6A-B). To further investigate the mechanisms of the antioxidative actions exerted by SFN, we measured the antioxidant defense system. Quantitative PCR analysis demonstrated that ethanol administration alone inhibited both Nrf2, Keap1, NQO-1, GPX1, SOD1 and SOD2 expression, but they were significantly increased in co-application of SFN and ethanol (Fig. 6C-H). The level of MDA was increased in ethanol treatment group, however co-application of SFN significantly reduced it compared with ethanol treatment alone (Fig. 6I). Furthermore, we examined the antioxidant enzymes in chick CAM. The level of GSH was increased and GSSG was decreased in ethanol treatment group, but co-application of SFN significantly increased GSH compared with ethanol treatment alone (Fig. 6J-K). Besides, the level of T-SOD was similar with the mRNA level of SOD1 and SOD2. This indicates that SFN administration can counteract ethanol-induced excessive ROS production in chick CAM.

We also detected the activities of ADH and ALDH, the key ethanol metabolism enzymes, in chick CAM and embryos. The results showed that ethanol increased the activity of ADH and decreased activity of ALDH compared with control group in chick embryos, and co-administration of SFN recovered their levels compared to normal control group. In chick CAM, SFN co-administration increased the activity of both ADH and ALDH (Fig. S3A-D).

Immunofluorescent staining of ATF6 and GRP78, the markers for endoplasmic reticulum (ER) stress [29], were carried out on the transverse sections of chick CAM exposed to SFN alone, ethanol alone or combination of both (Fig. 7A-H). The results showed that ethanol administration alone increased the expressions of GRP78 and ATP6 compared to control (arrows in C2 and G2), but this increase was not observed when SFN and ethanol were applied together (Fig. 7A1-D1, 7A2-D2, 7E1-H1, 7E2-H2). In order to quantify changes in protein and mRNA levels, Western blot (Fig. 7I) and quantitative PCR (Fig. 7J-K) were used to detect the expressions of GRP78 and IRE1 in chick CAM, and the results indicated that ethanol administration alone increased GRP78 (both protein and mRNA) and IRE1 (mRNA) expressions. The combinational application of SFN and ethanol significantly reduced ethanol-induced GRP78 and IRE1 expressions (Fig. 7I-K).

In order to further confirm the ER stress involvement, thapsigargin, a specific endoplasmic reticulum (ER) membrane Ca^{2+}-ATPase inhibitor [30], was applied to the chick CAM angiogenesis model (Fig. 8A-C). The results showed that the blood vessel density in CAM were reduced in the presence of thapsigargin, but recovered when

352 thapsigargin was applied with SFN (Fig. 8A1-C1). Likewise, we found that
353 thapsigargin administration alone reduced vascular plexus densities and
354 combinational application with SFN could recover this reduction of vascular plexus
355 densities (Fig. 8D). Quantitative PCR data showed that thapsigargin administration
356 alone increased the expressions of GRP78, ATF6 and IRE1 in chick CAM, and the
357 increased expressions of these genes significantly dropped when thapsigargin was
358 applied with SFN (Fig. 8E-G). These data suggest that ethanol exposure induces ER
359 stress, and SFN is able to remove the ER stress induced by ethanol exposure to some
360 extent.
361

Discussion

The fundamental function of embryonic yolk sac membrane (YSM), the extra embryonic membrane, is to absorb nutrition from yolk for developing embryos. YSM derive from blood islands and are full of vascular plexuses. They are also the sites of primary vessel growth, blood cell formation, lymphatic and germ cell proliferation. Chick chorioallantoic membrane (CAM) assays have been extensively employed to study the effects of chemical/compounds or detrimental factors on angiogenesis [26, 31]. Hence, both of the embryonic angiogenesis models were used here to study if SFN administration could reduce the teratogenic impact of alcohol on angiogenesis. First of all, the effect of SFN administration alone on angiogenesis was checked in both of models that lower concentration (less than 10 μM) of SFN stimulating angiogenesis and higher concentrations (more than 20 μM) inhibiting angiogenesis (Fig. 1-2). HUVECs tube formation model confirmed that the lower concentration SFN could reduce the negative impact of ethanol (Fig. S2). The concentrations of the SFN, which stimulating angiogenesis in chick YSM and CAM, were higher than the ones used in our *in vitro* experiments[18-19, 32]. This might be due to the diversity and absorptivity between *in vivo* and *in vitro* approaches, since the *in vivo* microenvironment of YSM and CAM are certainly more complicated than one at incubated one layer of cells *in vitro*. Even the same concentration of SFN presented some different effects on stimulating angiogenesis or anti-angiogenesis when the different endothelial cell lines are employed. For instance, Bertl *et al*. demonstrated that even 0.1 μM SFN (lower concentrations compared other applications) could suppress the formation of novel

384 micro-capillaries using an *in vitro* anti-angiogenesis model (Human microvascular
385 endothelial cells)[33]. However, most studies showed more than 10μM SFN could
386 suppress angiogenesis *in vitro (*HUVECs and Bovine aortic endothelial cells*)*[18-19, 32-36]
387 and *in vivo* (Balb/C mice implanted with VEGF-impregnated Matrigel plugs)[34]
388 experiments. Our observations are generally similar to the experimental results in
389 those literatures.

390 Based on the aforementioned data and our previous results, 5 or 10 μM SFN with
391 ethanol were administered together in chick YSM and CAM angiogenesis models, in
392 which the ethanol-repressed angiogenesis in both of the models were restored by
393 addition of SFN in a dose- and time-dependent manner (Fig. 3-4). In a previous study,
394 ethanol and ethanol-induced ROS were demonstrated to negatively affect the
395 expression of angiogenesis-related genes during chick embryo development, including
396 VEGF and FGF2 [10]. In this study, the combinational application of ethanol and SFN
397 dramatically increased expressions of VEGFa and FGF2 in chick CAM (Fig. 4).

398 There are two possible mechanisms for the effect of SFN on angiogenesis by the
399 combinational application of SFN with ethanol. Firstly, it is mainly because SFN
400 directly influences on the expressions of angiogenesis-related genes. For instance,
401 more than 5μM and 10μM SFN could inhibit HIF-1α and VEGF expression in cancer
402 cells *in vitro*[37]. We also found that the treatment of SFN (lower than 5μM) could
403 up-regulate thioredoxin reductase, and thioredoxin might contribute to facilitate the
404 effect on angiogenesis at the low dose[38]. Up-regulation of TR-1 can promote VEGF
405 expression[39]. Secondly, it also could due to SFN's antioxidant activity, which

406 neutralizes the ethanol exposure-induced excessive ROS production or inhibits
407 anti-oxidative gene expressions. The latter is more plausible since SFN has previously
408 been reported as an antioxidant[1].

409 In both our previous and this study (Fig. 5), we discovered that ethanol-exposure
410 could increase cell apoptosis in chick CAM, and additional administration of SFN
411 significantly reversed ethanol-increased cell apoptosis/necrosis (Fig. 5). Furthermore,
412 the possible pathological mechanisms of SFN were explored in protection against cell
413 apoptosis/necrosis in chick CAM. Oxidative stress refers to the disruption of the
414 balance between the production of reactive oxygen species (ROS) and antioxidant
415 defenses. Interestingly, the production of ROS was dramatically increased when chick
416 CAM were exposed to either SFN or ethanol, but decreased significantly when
417 exposed to both SFN and ethanol together (Fig. 6A-B). In the nucleus, Nrf2 binds to
418 the regulatory sequences (5'-G(/A)TGAC(/G)nnnGCA(/C)-3'), termed antioxidant
419 responsive elements (AREs) located in the promoter region of genes encoding the
420 antioxidant and phase II detoxifying enzymes. NRF2 regulates more than 100 genes
421 including most antioxidant enzymes such as NQO-1, QR, UGTs, GCS, AKR, HO,
422 TrxR1, GPX2, catalase and SODs [23, 40]. Thus, the antioxygenation of SFN might
423 through the Nrf2 signaling (Fig. 6C-L). Ethanol is eliminated from the body by
424 various metabolic mechanisms, which including the aldehyde dehydrogenase (ALDH)
425 and alcohol dehydrogenase (ADH). SFN co-administration increased the activity of
426 both ADH and ALDH might be the other mechanisms of antioxygenation (Fig. S3).
427 This supports the observation that the combinational application of SFN and ethanol

428 could rescue ethanol-induced cell apoptosis in chick CAM.

429 ER misfolded protein accumulation causes an adaptive stress response, which is
430 regulated by ER transmembrane protein kinase and endoribonuclease
431 inositol-requiring enzyme-1alpha (IRE1α) [41]. The effect of ethanol induced cell death
432 may be mediated by the interaction between oxidative stress and ER stress [42]. It is
433 suggested that ER stress might be another or secondary factor to lead to the
434 aforementioned phenotype. In this study, ethanol exposure increased the expressions
435 of ATF6, GRP78 and IRE1, the ER stress markers [29, 43], and combinational application
436 of SFN and ethanol reduced their expressions in chick CAM (Fig. 7), implying that
437 SFN could alleviate ethanol-induced ER stress. Thapsigargin, a blocker of
438 endoplasmic reticulum Ca^{2+} pump [30, 44], was employed to further verify the
439 involvement of ER stress in chick CAM since thapsigargin could induce ER stress [45].
440 The results (Fig. 8) demonstrated that thapsigargin alone suppressed angiogenesis,
441 which reflects in the reduction of vascular plexus densities in chick CAM, and
442 up-regulated the expressions of ATF6, GRP78 and IRE1, and the experimental results
443 were completely reversed when thapsigargin and SFN were applied together, thus
444 reconfirming the importance of ER stress during the protection of SFN in
445 ethanol-induced apoptosis.

446 In summary, we found that appropriate concentrations of SFN could rescue
447 ethanol-repressed embryonic angiogenesis. This may be achieved through alleviating
448 the inhibition of angiogenesis-related gene expression induced by ethanol exposure.
449 However, a potential more important defense mechanism is that SFN ameliorates

excessive ROS production and ER stress, thereby reducing the cell apoptosis in chick CAM, which will benefit embryo angiogenesis as a whole (Fig. 9). More studies should focus on the biphasic effects and individual differences of SFN on angiogenesis in the future. Anyway, our study suggested that SFN, in an appropriate concentration, could be a potential candidate compound for preventing the negative impact of alcohol on angiogenesis.

Acknowledgements

This study was supported by NSFC grant (31771331,81741016), Science and Technology Planning Project of Guangdong Province (2017A050506029, 2017A020214015, 2016B030229002), Science and Technology Program of Guangzhou (201710010054), Guangdong Natural Science Foundation (2016A030311044), The Fundamental Research Funds for the Central Universities (21617466).

Author Contributions

G.W. and J.N. performed the experiments and collected the data. Y.B. and X.Y. contributed to the design of the experiments, and wrote up the manuscript.

References

1. Chen, X.; Liu, J.; Chen, S. Y. Sulforaphane protects against ethanol-induced oxidative stress and apoptosis in neural crest cells by the induction of Nrf2-mediated antioxidant response. *Br J Pharmacol*. **2013,** *169*, 437-448.

2. Mead, E. A.; Sarkar, D. K. Fetal alcohol spectrum disorders and their transmission through genetic and epigenetic mechanisms. *Front Genet*. **2014,** *5*, 154.

3. Li, X.; Gao, A.; Wang, Y.; Chen, M.; Peng, J.; Yan, H.; Zhao, X.; Feng, X.; Chen, D. Alcohol exposure leads to unrecoverable cardiovascular defects along with edema and motor function changes in developing zebrafish larvae. *Biol Open*. **2016,** *5*, 1128-1133.

4. Chung, A. S.; Ferrara, N. Developmental and pathological angiogenesis. *Annu Rev Cell Dev Biol*. **2011,** *27*, 563-584.

5. Patan, S. Vasculogenesis and angiogenesis. *Cancer Treat Res*. **2004,** *117*, 3-32.

6. Holmes, D. I.; Zachary, I. The vascular endothelial growth factor (VEGF) family: angiogenic factors in health and disease. *Genome Biol*. **2005,** *6*, 209.

7. Cao, R.; Brakenhielm, E.; Pawliuk, R.; Wariaro, D.; Post, M. J.; Wahlberg, E.; Leboulch, P.; Cao, Y. Angiogenic synergism, vascular stability and improvement of hind-limb ischemia by a combination of PDGF-BB and FGF-2. *Nat Med*. **2003,** *9*, 604-613.

8. Lee, S. L.; Rouhi, P.; Dahl Jensen, L.; Zhang, D.; Ji, H.; Hauptmann, G.; Ingham, P.; Cao, Y. Hypoxia-induced pathological angiogenesis mediates tumor cell dissemination, invasion, and metastasis in a zebrafish tumor model. *Proc Natl Acad*

493 *Sci U S A.* **2009,** *106*, 19485-19490.

494 9. Dace, D. S.; Khan, A. A.; Kelly, J.; Apte, R. S. Interleukin-10 promotes
495 pathological angiogenesis by regulating macrophage response to hypoxia during
496 development. *PLoS One.* **2008,** *3*, e3381.

497 10. Wang, G.; Zhong, S.; Zhang, S. Y.; Ma, Z. L.; Chen, J. L.; Lu, W. H.; Cheng, X.;
498 Chuai, M.; Lee, K. K.; Lu, D. X.; Yang, X. Angiogenesis is repressed by ethanol
499 exposure during chick embryonic development. *J Appl Toxicol.* **2016,** *36*, 692-701.

500 11. Giordano, F. J. Oxygen, oxidative stress, hypoxia, and heart failure. *J Clin Invest.*
501 **2005,** *115*, 500-508.

502 12. Sawyer, D. B.; Siwik, D. A.; Xiao, L.; Pimentel, D. R.; Singh, K.; Colucci, W. S.
503 Role of oxidative stress in myocardial hypertrophy and failure. *J Mol Cell Cardiol.*
504 **2002,** *34*, 379-388.

505 13. Murdoch, C. E.; Zhang, M.; Cave, A. C.; Shah, A. M. NADPH oxidase-dependent
506 redox signalling in cardiac hypertrophy, remodelling and failure. *Cardiovasc Res.*
507 **2006,** *71*, 208-215.

508 14. Valko, M.; Leibfritz, D.; Moncol, J.; Cronin, M. T.; Mazur, M.; Telser, J. Free
509 radicals and antioxidants in normal physiological functions and human disease. *Int J*
510 *Biochem Cell Biol.* **2007,** *39*, 44-84.

511 15. Malhotra, J. D.; Kaufman, R. J. Endoplasmic reticulum stress and oxidative stress:
512 a vicious cycle or a double-edged sword? *Antioxid Redox Signal.* **2007,** *9*, 2277-2293.

513 16. Karbownik, M.; Lewinski, A. The role of oxidative stress in physiological and
514 pathological processes in the thyroid gland; possible involvement in pineal-thyroid

515 interactions. *Neuro Endocrinol Lett.* **2003,** *24*, 293-303.

516 17. Singal, P. K.; Bello-Klein, A.; Farahmand, F.; Sandhawalia, V. Oxidative stress
517 and functional deficit in diabetic cardiomyopathy. *Adv Exp Med Biol.* **2001,** *498*,
518 213-220.

519 18. Bao, Y.; Wang, W.; Zhou, Z.; Sun, C. Benefits and risks of the hormetic effects of
520 dietary isothiocyanates on cancer prevention. *PLoS One.* **2014,** *9*, e114764.

521 19. Liu, P.; Atkinson, S. J.; Akbareian, S. E.; Zhou, Z.; Munsterberg, A.; Robinson, S.
522 D.; Bao, Y. Sulforaphane exerts anti-angiogenesis effects against hepatocellular
523 carcinoma through inhibition of STAT3/HIF-1alpha/VEGF signalling. *Sci Rep.* **2017,**
524 *7*, 12651.

525 20. Keum, Y. S.; Jeong, W. S.; Kong, A. N. Chemopreventive functions of
526 isothiocyanates. *Drug News Perspect.* **2005,** *18*, 445-451.

527 21. Hong, F.; Freeman, M. L.; Liebler, D. C. Identification of sensor cysteines in
528 human Keap1 modified by the cancer chemopreventive agent sulforaphane. *Chem Res*
529 *Toxicol.* **2005,** *18*, 1917-1926.

530 22. Thimmulappa, R. K.; Mai, K. H.; Srisuma, S.; Kensler, T. W.; Yamamoto, M.;
531 Biswal, S. Identification of Nrf2-regulated genes induced by the chemopreventive
532 agent sulforaphane by oligonucleotide microarray. *Cancer Res.* **2002,** *62*, 5196-5203.

533 23. Lei, X. G.; Zhu, J. H.; Cheng, W. H.; Bao, Y.; Ho, Y. S.; Reddi, A. R.; Holmgren,
534 A.; Arner, E. S. Paradoxical Roles of Antioxidant Enzymes: Basic Mechanisms and
535 Health Implications. *Physiol Rev.* **2016,** *96*, 307-364.

536 24. Wang, W.; He, Y.; Yu, G.; Li, B.; Sexton, D. W.; Wileman, T.; Roberts, A. A.;

537 Hamilton, C. J.; Liu, R.; Chao, Y.; Shan, Y.; Bao, Y. Sulforaphane Protects the Liver
538 against CdSe Quantum Dot-Induced Cytotoxicity. *PLoS One*. **2015,** *10*, e0138771.
539 25. He, Y. Q.; Li, Y.; Wang, X. Y.; He, X. D.; Jun, L.; Chuai, M.; Lee, K. K.; Wang, J.;
540 Wang, L. J.; Yang, X. Dimethyl phenyl piperazine iodide (DMPP) induces glioma
541 regression by inhibiting angiogenesis. *Exp Cell Res*. **2014,** *320*, 354-364.
542 26. Cheng, X.; Luo, R.; Wang, G.; Xu, C. J.; Feng, X.; Yang, R. H.; Ding, E.; He, Y.
543 Q.; Chuai, M.; Lee, K. K.; Yang, X. Effects of 2,5-hexanedione on angiogenesis and
544 vasculogenesis in chick embryos. *Reprod Toxicol*. **2015,** *51*, 79-89.
545 27. Maroto, M.; Reshef, R.; Munsterberg, A. E.; Koester, S.; Goulding, M.; Lassar, A.
546 B. Ectopic Pax-3 activates MyoD and Myf-5 expression in embryonic mesoderm and
547 neural tissue. *Cell*. **1997,** *89*, 139-148.
548 28. Dugaiczyk, A.; Haron, J. A.; Stone, E. M.; Dennison, O. E.; Rothblum, K. N.;
549 Schwartz, R. J. Cloning and sequencing of a deoxyribonucleic acid copy of
550 glyceraldehyde-3-phosphate dehydrogenase messenger ribonucleic acid isolated from
551 chicken muscle. *Biochemistry*. **1983,** *22*, 1605-1613.
552 29. Shen, J.; Chen, X.; Hendershot, L.; Prywes, R. ER stress regulation of ATF6
553 localization by dissociation of BiP/GRP78 binding and unmasking of Golgi
554 localization signals. *Dev Cell*. **2002,** *3*, 99-111.
555 30. Lytton, J.; Westlin, M.; Hanley, M. R. Thapsigargin inhibits the sarcoplasmic or
556 endoplasmic reticulum Ca-ATPase family of calcium pumps. *J Biol Chem*. **1991,** *266*,
557 17067-17071.
558 31. Richardson, M.; Singh, G. Observations on the use of the avian chorioallantoic

membrane (CAM) model in investigations into angiogenesis. *Curr Drug Targets Cardiovasc Haematol Disord.* **2003,** *3*, 155-185.

32. Wang, Y.; Zhou, Z.; Wang, W.; Liu, M.; Bao, Y. Differential effects of sulforaphane in regulation of angiogenesis in a co-culture model of endothelial cells and pericytes. *Oncol Rep.* **2017,** *37*, 2905-2912.

33. Bertl, E.; Bartsch, H.; Gerhauser, C. Inhibition of angiogenesis and endothelial cell functions are novel sulforaphane-mediated mechanisms in chemoprevention. *Mol Cancer Ther.* **2006,** *5*, 575-585.

34. Jackson, S. J.; Singletary, K. W.; Venema, R. C. Sulforaphane suppresses angiogenesis and disrupts endothelial mitotic progression and microtubule polymerization. *Vascul Pharmacol.* **2007,** *46*, 77-84.

35. Nishikawa, T.; Tsuno, N. H.; Okaji, Y.; Sunami, E.; Shuno, Y.; Sasaki, K.; Hongo, K.; Kaneko, M.; Hiyoshi, M.; Kawai, K.; Kitayama, J.; Takahashi, K.; Nagawa, H. The inhibition of autophagy potentiates anti-angiogenic effects of sulforaphane by inducing apoptosis. *Angiogenesis.* **2010,** *13*, 227-238.

36. Davis, R.; Singh, K. P.; Kurzrock, R.; Shankar, S. Sulforaphane inhibits angiogenesis through activation of FOXO transcription factors. *Oncol Rep.* **2009,** *22*, 1473-1478.

37. Kim, D. H.; Sung, B.; Kang, Y. J.; Hwang, S. Y.; Kim, M. J.; Yoon, J. H.; Im, E.; Kim, N. D. Sulforaphane inhibits hypoxia-induced HIF-1alpha and VEGF expression and migration of human colon cancer cells. *Int J Oncol.* **2015,** *47*, 2226-2232.

38. Bacon, J. R.; Plumb, G. W.; Howie, A. F.; Beckett, G. J.; Wang, W.; Bao, Y. Dual

581 action of sulforaphane in the regulation of thioredoxin reductase and thioredoxin in
582 human HepG2 and Caco-2 cells. *J Agric Food Chem.* **2007,** *55*, 1170-1176.
583 39. Streicher, K. L.; Sylte, M. J.; Johnson, S. E.; Sordillo, L. M. Thioredoxin
584 reductase regulates angiogenesis by increasing endothelial cell-derived vascular
585 endothelial growth factor. *Nutr Cancer.* **2004,** *50*, 221-231.
586 40. Hayes, J. D.; McMahon, M. NRF2 and KEAP1 mutations: permanent activation
587 of an adaptive response in cancer. *Trends Biochem Sci.* **2009,** *34*, 176-188.
588 41. Hetz, C.; Bernasconi, P.; Fisher, J.; Lee, A. H.; Bassik, M. C.; Antonsson, B.;
589 Brandt, G. S.; Iwakoshi, N. N.; Schinzel, A.; Glimcher, L. H.; Korsmeyer, S. J.
590 Proapoptotic BAX and BAK modulate the unfolded protein response by a direct
591 interaction with IRE1alpha. *Science.* **2006,** *312*, 572-576.
592 42. Chen, G.; Ma, C.; Bower, K. A.; Shi, X.; Ke, Z.; Luo, J. Ethanol promotes
593 endoplasmic reticulum stress-induced neuronal death: involvement of oxidative stress.
594 *J Neurosci Res.* **2008,** *86*, 937-946.
595 43. Tay, K. H.; Luan, Q.; Croft, A.; Jiang, C. C.; Jin, L.; Zhang, X. D.; Tseng, H. Y.
596 Sustained IRE1 and ATF6 signaling is important for survival of melanoma cells
597 undergoing ER stress. *Cell Signal.* **2014,** *26*, 287-294.
598 44. Thastrup, O.; Cullen, P. J.; Drobak, B. K.; Hanley, M. R.; Dawson, A. P.
599 Thapsigargin, a tumor promoter, discharges intracellular Ca2+ stores by specific
600 inhibition of the endoplasmic reticulum Ca2(+)-ATPase. *Proc Natl Acad Sci U S A.*
601 **1990,** *87*, 2466-2470.
602 45. Janyou, A.; Changtam, C.; Suksamrarn, A.; Tocharus, C.; Tocharus, J.

603 Suppression effects of O-demethyldemethoxycurcumin on thapsigargin triggered on
604 endoplasmic reticulum stress in SK-N-SH cells. *Neurotoxicology*. **2015,** *50*, 92-100.

605

606

607 **Figure legends**

608 ***Fig 1. Assessing angiogenesis on chick embryo YSM following the treatment with***
609 ***various concentrations of SFN.***

610 **A**:The embryo pattern diagram illustrate show to implement either SFN or
611 DMSO (control) on chick embryo YSM (yolk sac membrane) and then quantitatively
612 measure angiogenesis. **B-G3**:The representative bright-field images of the leading
613 edges of vascular plexuses on chick embryo YSM were taken from control (B-B3),
614 2.5 μM SFN (C-C3), 5 μM SFN (D-D3), 10 μM SFN (E-E3), 20 μM SFN (F-F3) and
615 40 μM SFN (G-G3) group at 0-hour (B-G), 12-hour (B1-G1), 24-hour (B2-G2) and
616 36-hour (B3-G3) incubation. **H**:Bar chart showing the comparison of vascular plexus
617 densities on YSM of the chick embryos incubated different time among control and
618 various SFN concentrations groups. **$p<0.01$, ***$p<0.001$ compared with control
619 group. Scale bars = 5 mm in A and 2 mm in B-G3.

620

621 ***Fig 2. Assessing angiogenesis on CAM and chick embryo mortality following the***
622 ***treatment with various concentrations of SFN.***

623 **A**:The sketches illustrate how and when to implement either SFN or DMSO
624 (control) injection and embryo harvests in fertilized eggs. **B-C**:Bar charts showing the

comparison of embryos' weight (B) and mortalities (C) of the day 9 (E9.0) chick embryos among control and various SFN concentrations groups. **D**:The representative bright-field images of vascular plexuses on chick embryo CAM (chorioallantoic membrane) were taken from control, 2.5 μM SFN, 5 μM SFN, 10 μM SFN group. **E**:Bar charts showing the comparison of vascular plexus densities on chick CAM of the day 9 (E9.0) chick embryos among control and various SFN concentrations groups. *p<0.05, **p<0.01, ***p<0.001 compared with control group. Abbreviation: Ctrl, Control. Scale bars = 5 mm in D.

Fig 3. Assessing angiogenesis on chick embryo YSM following the treatment with ethanol and various concentrations of SFN.

A: The embryo pattern diagram illustrates how to implement either ethanol and SFN or DMSO (control) on chick embryo YSM (yolk sac membrane) and then quantitatively measure angiogenesis. **B-G3**:The representative bright-field images of the leading edges of vascular plexuses on chick embryo YSM were taken from control (B-B3), 5 μM SFN (C-C3), 10 μM SFN (D-D3), 15% ethanol (E-E3), 15% ethanol + 5 μM SFN (F-F3) and 15% ethanol + 10 μM SFN (G-G3) group at 0-hour (B-G), 12-hour (B1-G1), 24-hour (B2-G2) and 36-hour (B3-G3) incubation. **H**: Bar chart showing the comparison of vascular plexus densities on YSM of the chick embryos incubated different time among control, SFN only, ethanol only and SFN + ethanol groups. *p<0.05, **p<0.01, ***p<0.001 compared with control group; $^{\#\#}$p<0.01, $^{\#\#\#}$p<0.001 compared with ethanol group. Abbreviation: EtOH, Ethanol. Scale bars =

5 mm in A and 2 μm in B-G3.

Fig 4. Assessing angiogenesis on chick embryo CAM following the treatment with ethanol and various concentrations of SFN.

A-D, **A1-D1**:The representative bright-field images of the vascular plexuses on chick embryo CAM were taken from control (A-A1), 10 μM SFN (B-B1), 15% ethanol (C-C1) and 15% ethanol + 10 μM SFN (D-D1) group. A1-D1 are the high magnification images from the sites indicated by dotted squares in A-D respectively. **E-G**:Bar charts showing the comparison of embryos' weight (E), mortalities (F) and vascular plexus densities (G) on chick embryo CAM among control, SFN or ethanol only, and SFN + ethanol groups. **H-K**:The representative H&E stained transverse sections from the sites indicated by dotted lines in A1-D1 respectively. **L-O**:Cav1 immunofluorescent staining was implemented on the transverse sections from the sites indicated by dotted lines in A1-D1 respectively before applying the DAPI counterstain. **P**:Bar charts showing the comparison of blood vessel diameter on chick embryo CAM among control, SFN or ethanol only, and SFN + ethanol groups. **Q-S**:Bar charts showing the quantitative PCR data about the expressions of VEGFa (Q), FGF2 (R) and HIF1α (S) in chick embryo CAM among control, SFN or ethanol only, and SFN + ethanol groups. *$p<0.05$, **$p<0.01$, ***$p<0.001$ compared with control group; $^{\#\#}p<0.01$, $^{\#\#\#}p<0.001$ compared with ethanol group. Abbreviations: EtOH, Ethanol. Scale bars = 5 mm in A-D; 2 mm in A1-D1; 50 μm in H-K and 100 μm in L-O.

669

670 ***Fig 5. Determining cell apoptosis on chick embryo CAM following the treatment***
671 ***with ethanol and SFN.***

672 **A-D**:TUNEL (terminal deoxynucleotidyl transferase-mediated dUTP nick-end
673 labeling) staining was implemented on the transverse sections at the same orientation
674 of chick CAM from control (A), 10 μM SFN only (B), 15% ethanol only (C), and 10
675 μM SFN + 15% ethanol (D) group before applying the hematoxylin counterstain.
676 **A1-D1**:The high magnification images from the sites indicated by dotted squares in
677 A-D respectively. **E**:Bar chart showing the percentages of TUNEL-positive cells in
678 chick embryo CAM among control, 10 μM SFN only, 15% ethanol only, and 10 μM
679 SFN + 15% ethanol groups. **F**:The Annexin V/PI (propidium iodide) flowcytometric
680 assay was implemented in mentioned-above groups. **G**:Bar charts showing the
681 percentages of apoptotic positive necrotic cells revealed by flow cytometry analysis
682 stained with Annexin V/PI in chick embryo CAM among mentioned-above groups.
683 *$p<0.05$, **$p<0.01$, ***$p<0.001$ compared with control group; $^{\#}p<0.05$, $^{\#\#\#}p<0.001$
684 compared with ethanol group. Abbreviations: EtOH, Ethanol. Scale bars = 50 μm in
685 A-D and 20 μm in A1-D1.

686

687 ***Fig 6. Determining ROS production on chick embryo CAM following the treatment***
688 ***with ethanol and various concentrations of SFN.***

689 **A-B**:Flow cytometry and bar charts showing the percentages of ROS production
690 in chick embryo CAM among control, 5 μM SFN (A) or 10 μM SFN (B) only, 15%

ethanol only, and SFN + ethanol groups. **C-H**:Bar charts showing quantitative PCR data about the relative quantity of Nrf2 (C), Keap1 (D), NQO-1 (E), GPX1 (F), SOD1 (G) and SOD2 (H) expressions (normalized to GAPDH) in chick embryo CAM among control, 10 μM SFN only, 15% ethanol only and 10 μM SFN + 15% ethanol groups. I-**L**: The levels of MDA (I), GSH (J), GSSG (K) and the activity of T-SOD (L) in chick embryo CAM among control, 10 μM SFN only, 15% ethanol only and 10 μM SFN + 15% ethanol groups. *$p<0.05$, **$p<0.01$, ***$p<0.001$ compared with control group; $^{\#\#}p<0.01$, $^{\#\#\#}p<0.001$ compared with ethanol group. Abbreviations: EtOH, Ethanol.

Fig 7. Determining GRP78 and ATF6 expressions on chick embryo CAM following the treatment with ethanol and SFN.

A-D:GRP78 immunofluorescent staining was implemented on the transverse sections at the same orientation of chick CAM from control (A), 10 μM SFN only (B), 15% ethanol only (C), and 10 μM SFN + 15% ethanol (D) group before applying the DAPI counterstain. **A1-D1, A2-D2**:A1-D1 are the high magnification images of GRP78 expression only from the sites indicated by dotted squares in A-D respectively. A2-D2 are the DAPI counterstain in A1-D1 respectively. **E-H**:ATF6 immunofluorescent staining was implemented on the transverse sections at the same orientation of chick CAM from control (E), 10 μM SFN only (F), 15% ethanol only (G), and 10 μM SFN + 15% ethanol (H) group before applying the DAPI counterstain. **E1-H1, E2-H2**:E1-H1 are the high magnification images of ATF6 expression only

from the sites indicated by dotted squares in E-H respectively. E2-H2 are the DAPI counterstain in E1-H1 respectively. **I**:Western blot data show the GRP78 expressions (arbitrary unit: normalized to β-actin) in chick embryo CAM among control, 10 μM SFN only, 15% ethanol only and 10 μM SFN + 15% ethanol groups. **J-K**:Bar charts showing quantitative PCR data about the relative quantity of GRP78 (J) and IRE1 (K) expressions (normalized to GAPDH) in chick embryo CAM among control, 10 μM SFN only, 15% ethanol only and 10 μM SFN + 15% ethanol groups. *p<0.05, **p<0.01, ***p<0.001 compared with control group; $^{\#}$p<0.05, $^{\#\#\#}$p<0.001 compared with ethanol group. Abbreviations: EtOH, Ethanol. Scale bars = 50 μm in A-H and 20 μm in A1-H1, A2-H2.

Fig 8. Assessing angiogenesis on chick embryo CAM following the treatment with thapsigargin and SFN.

A-C:The representative bright-field images of the vascular plexuses on chick embryo CAM were taken from control(A), 1 μM thapsigargin (B) and 1 μM thapsigargin + 10 μM SFN (C) group. A1-C1 are the high magnification images from the sites indicated by dotted squares in A-C respectively. **D**:Bar chart showing the comparison of relative vascular plexus densities (%) in chick embryo CAM among control, thapsigargin only, thapsigargin and SFN groups. **E-G**:Bar charts showing quantitative PCR data about the relative quantity of GRP78 (E), ATF6 (F) and IRE1 (G) expressions (normalized to GAPDH) in chick embryo CAM among control, thapsigargin only, thapsigargin and SFN groups. *p<0.05, **p<0.01, ***p<0.001

735 compared with control group; $^{\#}p<0.05$, $^{\#\#}p<0.01$, $^{\#\#\#}p<0.001$ compared with ethanol
736 group. Abbreviations: TG, Thapsigargin. Scale bars = 5 mm in A-C and 2 mm in
737 A1-C1.
738
739 ***Fig 9. Proposed mechanism illustrating how SFN ameliorates the ethanol-induced***
740 ***pathological angiogenesis.***
741
742 ***Supplementary Fig 1. The sets of primers used for RT-PCR and quantitative PCR in***
743 ***this study.***
744
745 ***Supplementary Fig 2. Effects of ethanol and/or SFN on endothelial tube formation***
746 ***in a 3-D angiogenesis assay.*** **A-H:** Representative images of tube formation of
747 Control, SFN, ethanol, ethanol + SFN groups in 4 h (A-D) and 8 h (E-H). **I-L**:CD31
748 immunofluorescent staining was implemented on the HUVECs from Control, SFN,
749 ethanol, ethanol + SFN before applying the DAPI counterstain. I1-L1 are the DAPI
750 counterstain in I-L respectively. **M:** Bar chart represents cumulative tube length of
751 3-D co-culture model exposed to ethanol and/or SFN. $^{*}p<0.05$, $^{***}p<0.001$ compared
752 with control group; $^{\#\#\#}p<0.001$ compared with ethanol group. Abbreviations: EtOH,
753 Ethanol. Scale bars = 200 μm in A-H and 200 μm in I-L, I1-L1.
754
755 ***Supplementary Fig 3. Ethanol metabolism pathway modified by SFN co-treatment***
756 ***might be involved in the protective effects against ethanol exposure on chick***

embryo CAM.

A-B: The activities of ADH in chick embryo (A) and CAM (B) among control, 10 μM SFN only, 15% ethanol only and 10 μM SFN + 15% ethanol groups. **C-D**: The activities of ALDH in chick embryo (C) and CAM (D) among control, 10 μM SFN only, 15% ethanol only and 10 μM SFN + 15% ethanol groups. *$p<0.05$, **$p<0.01$ compared with control group; $^{\#}p<0.05$, $^{\#\#\#}p<0.001$ compared with ethanol group. Abbreviations: Ctrl, Control; EtOH, Ethanol.

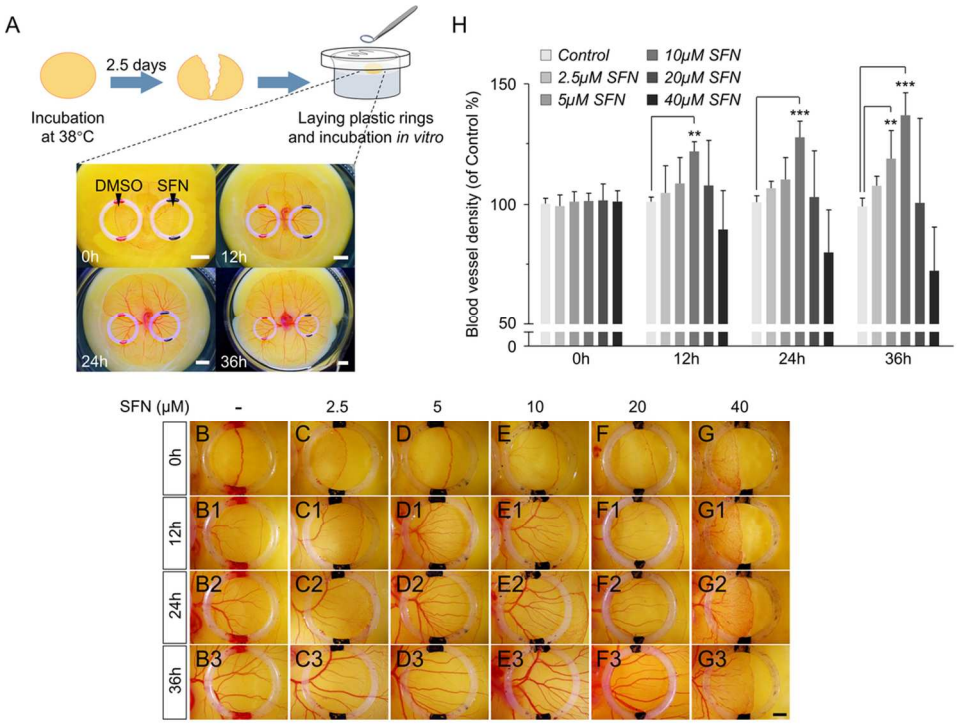

Figure 1

108x79mm (300 x 300 DPI)

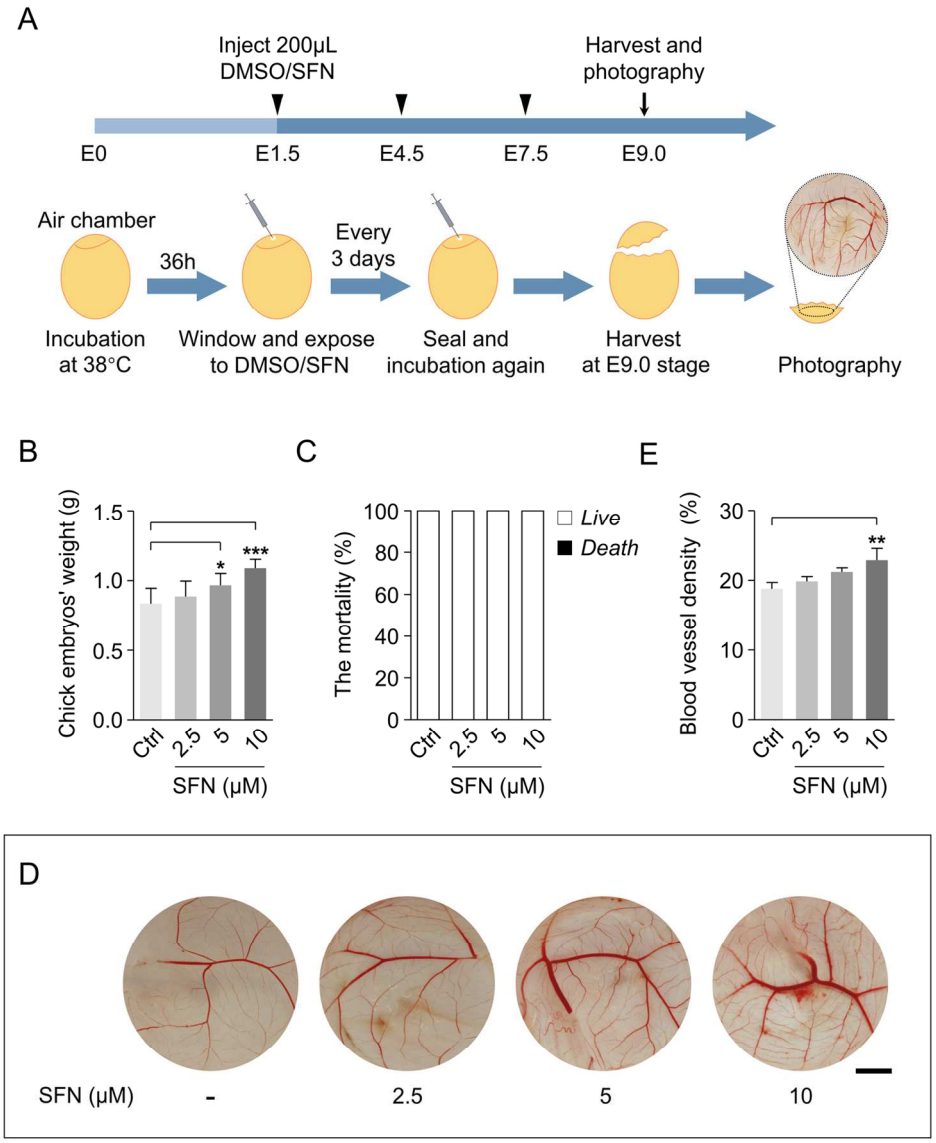

Figure 2

149x173mm (300 x 300 DPI)

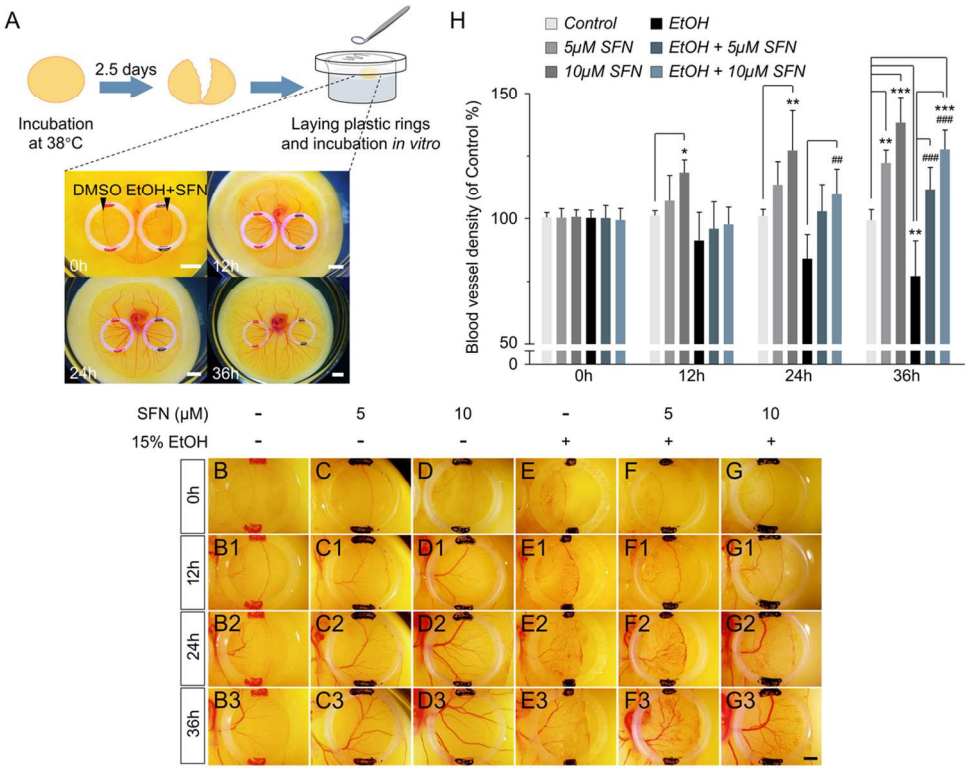

Figure 3

115x88mm (300 x 300 DPI)

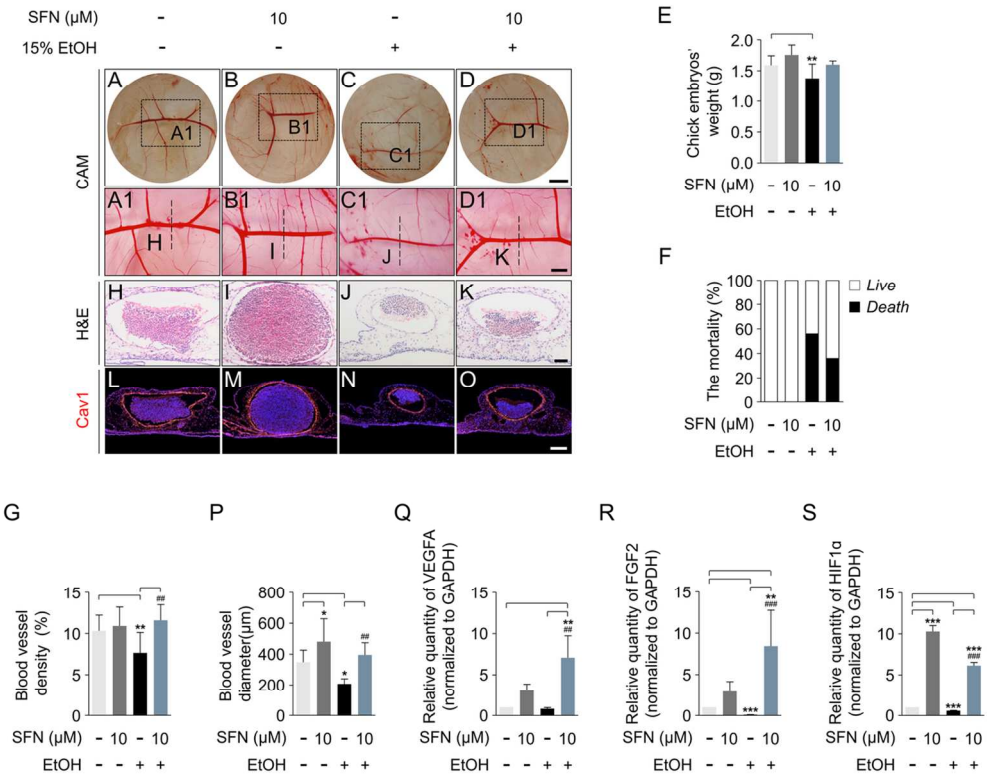

Figure 4

120x97mm (300 x 300 DPI)

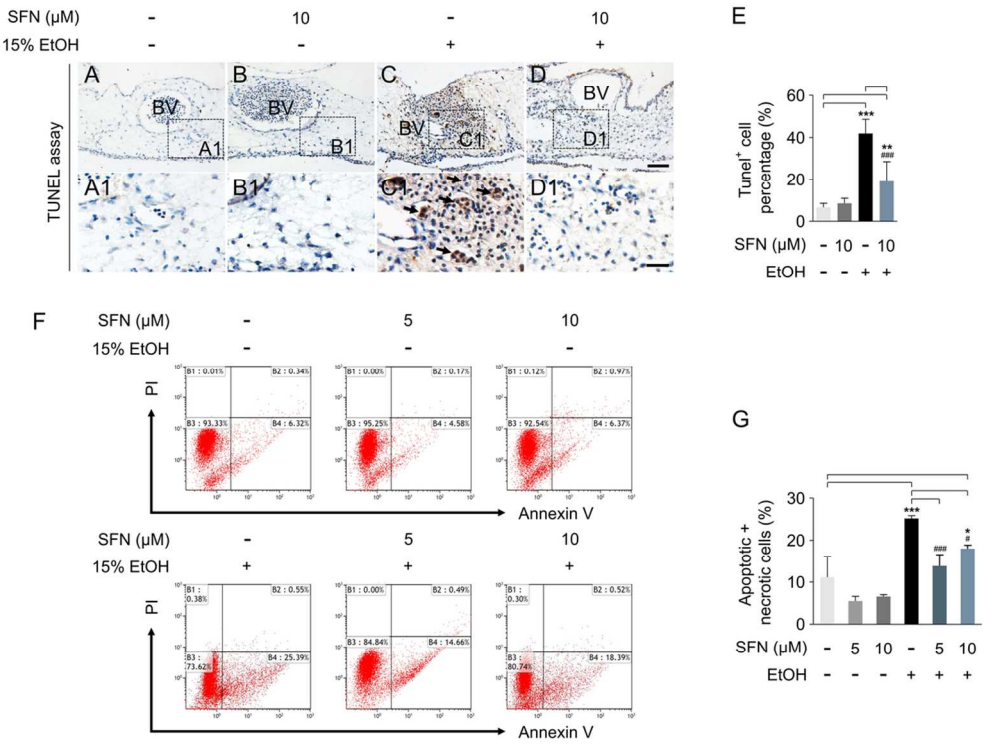

Figure 5

112x84mm (300 x 300 DPI)

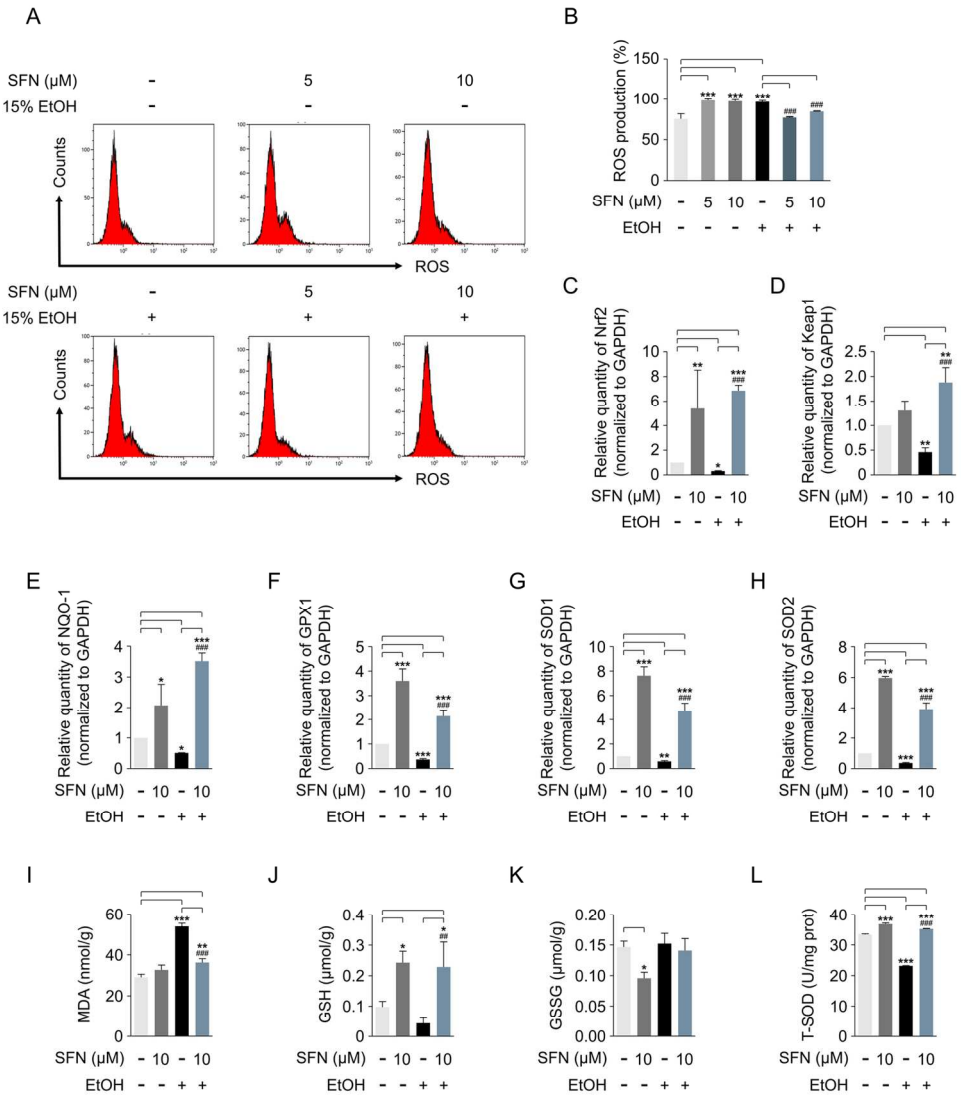

Figure 6

149x168mm (300 x 300 DPI)

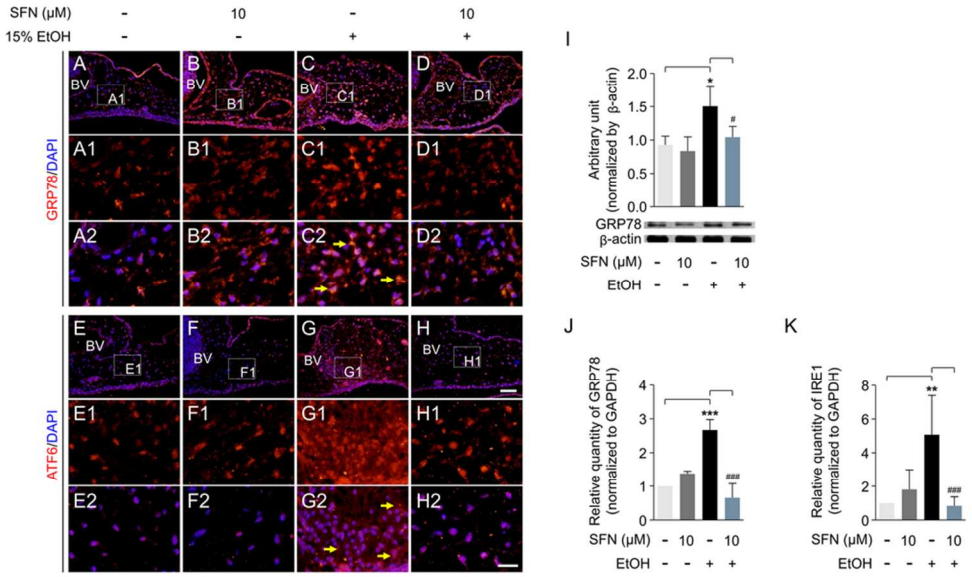

Figure 7

88x52mm (300 x 300 DPI)

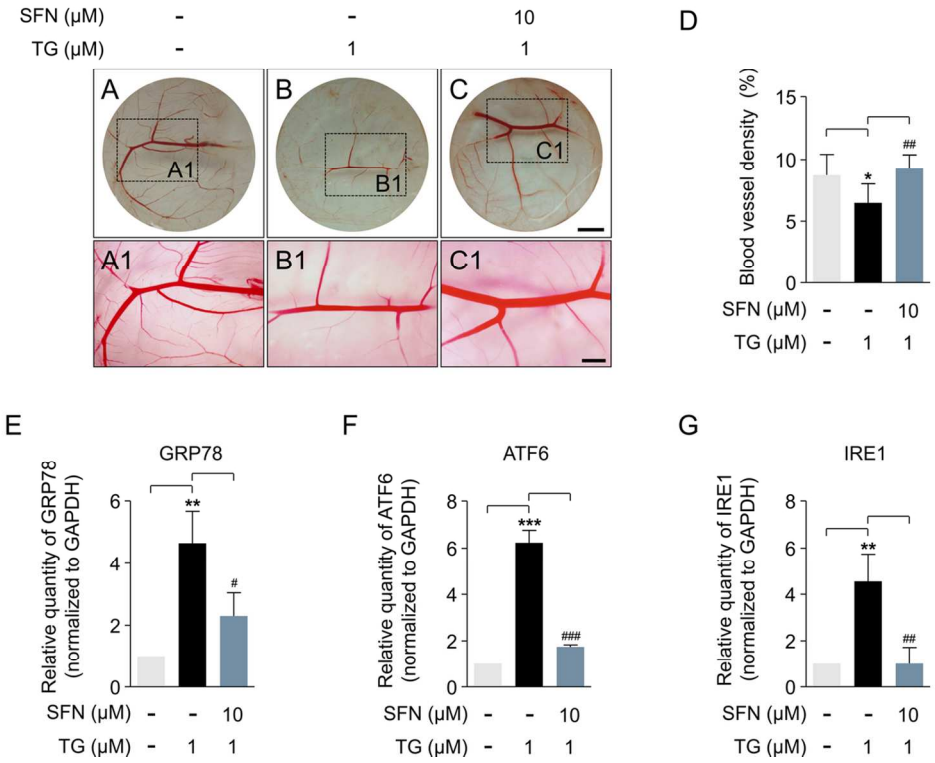

Figure 8

117x92mm (300 x 300 DPI)

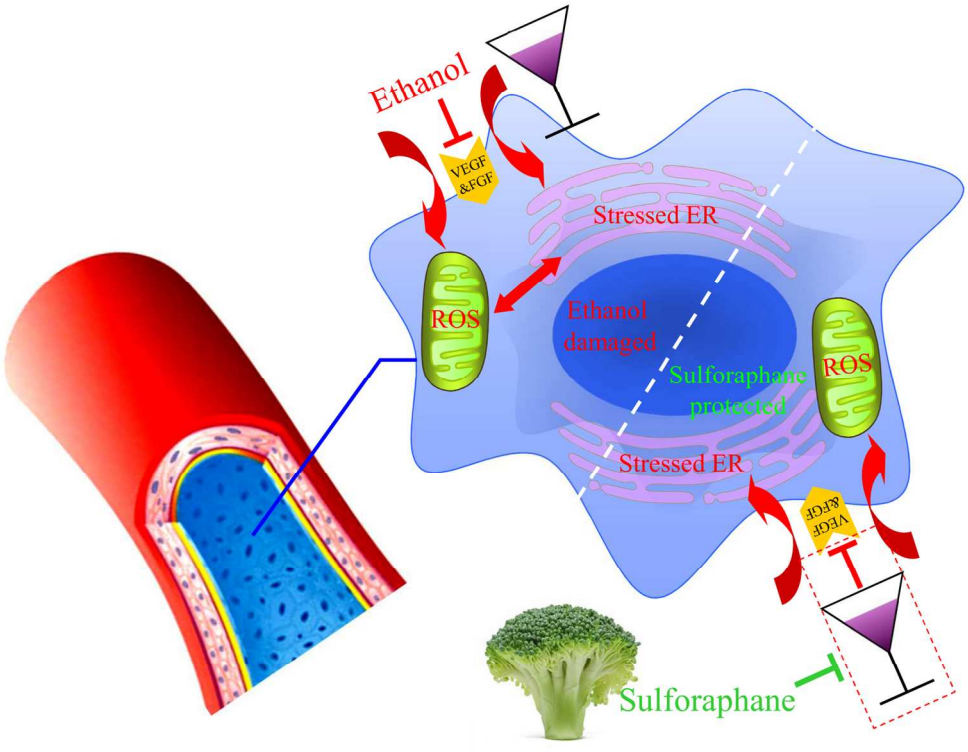

Figure 9

145x111mm (300 x 300 DPI)

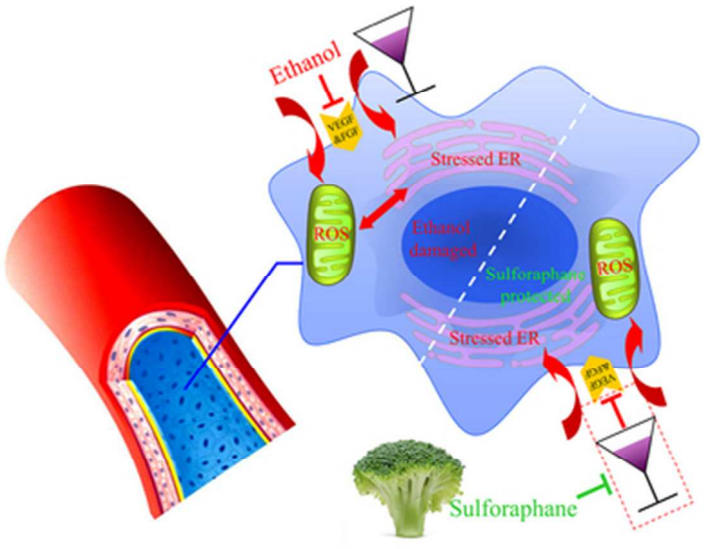

TOC Graphic

46x25mm (300 x 300 DPI)